

Enabling Live State-of-Health Monitoring for a Safety-Critical Automotive LiDAR System

Andreas Strasser[†], Philipp Stelzer[†], Christian Steger[†] and Norbert Druml^{*}

[†]Graz University of Technology, Graz, Austria

email:{strasser, stelzer, steger}@tugraz.at

^{*}Infineon Technologies Austria AG, Graz, Austria

email:{norbert.druml}@infineon.com

Abstract—In the next few years, modern vehicles will integrate the next level of Advanced Driver-Assistance Systems (ADAS) such as Light Detection and Ranging (LiDAR) which will be one of the key enabler for autonomous driving. Autonomous driving will be in charge for controlling the vehicle without any inputs of a passenger. This requires highly robust and reliable components and systems. In general, mechanical defects are detectable through vibrations or noise changes but for semiconductor components these capabilities are not available. Semiconductor components fail silently and abrupt without any prior information and this could lead to fatal accidents when systems fail during autonomous driving phases. In this publication, we are introducing a novel state-of-health monitoring system for automotive LiDAR system that is capable to economically record the component history and automatically processes these data to the statistical Failure-In-Time (FIT) Rate that is primarily used in the Automotive domain such as in the “ISO 26262 - Road Vehicle Safety” standard.

Index Terms—FIT Monitor, Reliability Monitor, Aging Monitor, LiDAR, Safety

I. INTRODUCTION

In the next decades, Smart Mobility will become more and more important for urban environments to manage environmental pollution, scarcity of raw materials and traffic congestion [1]. The amount of citizens that are using individual road vehicles to travel to work are steadily increasing and this causes extra costs for the individual as well as to the community. For this purpose, Smart Mobility applications such as car sharing or street light control are attempting to optimize the energy and resource usage as well as to reduce costs with the benefit of increasing the quality of life [2]. The next big hope in the area of Smart Mobility are autonomous vehicles. Autonomous vehicles have the capability of controlling the

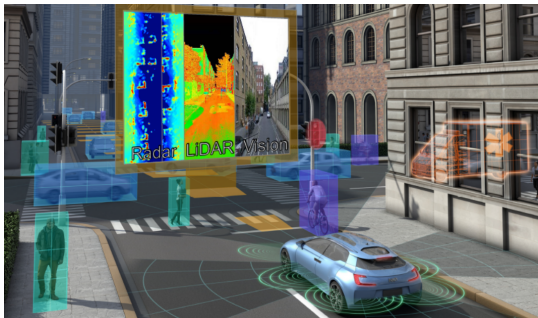


Fig. 1. PRYSTINE’s concept view of a fail-operational urban surround perception system [1].

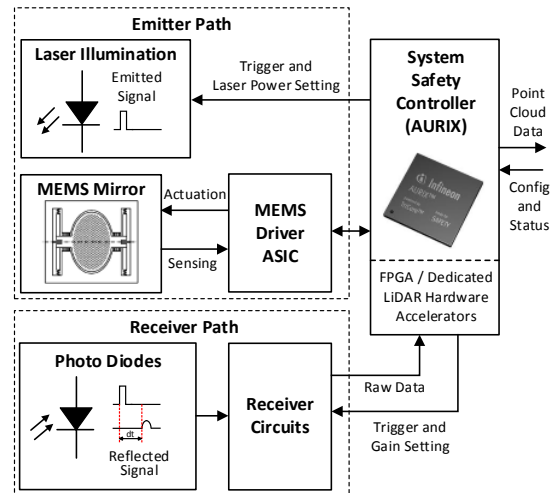


Fig. 2. Overview of a LiDAR system for autonomous driving [4].

vehicle independently without any intervention of a human person. This would enable citizens to call vehicles from car sharing companies that are autonomously driving to the pick-up address of the customer and drive them safely and comfortable to the destination address anytime and anywhere [3]. For enabling autonomous driving, next generation vehicles needs to be equipped with additional environmental perception sensors such as Radar, Light Detection and Ranging (LiDAR) and Vision Cameras to percept the proximity. One possible solution of such a perception system is PRYSTINE’s concept of a fail-operational urban surround perception system (FUSION) as depicted in Figure 1. The FUSION system combines the data of the individual Radar, LiDAR and Vision Cameras with sensor fusion and enables a safe and robust perception of other road participants [1]. Nowadays, there is no commercial middle-class car available that is equipped with a LiDAR system yet. One possible reason could be that traditional spinning mechanical LiDAR systems are quite expensive such as the Velodyne LiDAR system that still costs thousands of dollar but with optical phased array LiDAR systems the costs could be dropped to 250 US Dollar in larger volumes [5]. One possible solution of a robust low-cost automotive LiDAR system is the 1D MEMS Micro-Scanning LiDAR system as seen in Figure 2. The 1D MEMS Micro-Scanning LiDAR system from Druml et al. is a robust and safe automotive LiDAR system that will cost below 250 US Dollar and will

be the key enabler for autonomous driving functionalities in middle-class cars [4]. The system focus on highly robustness and safety and will achieve the Automotive Safety Integrity Level (ASIL) C.

In general, modern safety-critical automotive embedded systems are developed with high safety standards such as the ISO 26262 - Road Vehicle Safety standard [6]. But there is a drawback that the designers needs to determine a temperature mission profile which describes the estimated usage. Any major variation has a big influence on the reliability of the component such as higher reliability for lower temperature and lower reliability for higher temperature [7]. Both cases are not desirable due to higher manufacturing costs for the producer or less operation time for the customer. In worst case, safety-critical autonomous systems fail during operation and causes an accident. To prevent accidents that are caused by abrupt failing environmental perception systems such as LiDAR it would be preferable to monitor the lifetime usage of a component and detect and signalize overstressed microelectronic devices.

To prevent accidents that are caused by overstressed LiDAR components we want to contribute on the following research question:

- How can overstressed LiDAR components be detected during run-time and monitored the whole lifecycle efficiently?

II. RELATED WORKS

Safety and robustness is one of the most important key-factors for the overall acceptance of the next generation ADAS such as the FUSION platform of the PRYSTINE project [1]. The FUSION platform is able to percept the close environment of the vehicle and based on this data decisions for autonomous driving will be made. These decisions needs to be reliable because any mistake could lead to a fatal accident considering the vehicle is driving autonomously on a highway. To prevent fatal accidents, one possibility is to add redundancy and diversity to the overall system and increase the overall reliability but from an economical point-of-view it is not that simple [6]. Redundancy and diversity is mostly connected to higher costs and this results in less cost efficiency. To focus on the cost efficiency it would be preferable to detect failures before the overall system fails.

The correct functionality of a system is specified as Mean Time Between Failures (MTBF) and is a statistical value that indicates the time the system is able to perform without any present failure. The automotive domain is using the inverse value of the MTBF and is calling these value the Failure-In-Time (FIT) Rate. Based on the Automotive Safety Integrity Level (ASIL) that is derived from the Hazard and Risk Analysis (HARA), the FIT Rate of the system will be specified [6]. In general, the overall FIT Rate of systems can be determined by statistical field tests or specific reliability standards such as the IEC 62380 [8]. The IEC 62380 [8] and ISO 26262 [6], specifies that the reliability of hardware

components are temperature dependent and is expressed in the Arrhenius Equation as seen in (1).

$$DF = e^{\frac{E_a}{k} \cdot \left(\frac{1}{T_{use}} - \frac{1}{T_{stress}} \right)} \quad (1)$$

where:

- DF is Derating Factor
- E_a is Activation Energy in eV
- k is Boltzmann Constant (8.167303×10^{-5} ev/K)
- T_{use} is Use Junction Temperature in K
- T_{stress} is Stress Junction Temperature in K

The Derating Factor of the Arrhenius Equation is the key impact factor of the hardware component that is stressed by higher temperature and because of the exponential relation even slighty temperature increases should not be neglected. For that reason, temperature is one of the key factors for reliable hardware components and always had a special focus in the industry for safety-critical systems [6], [8].

Temperature affects the hardware components the most in terms of reliability and this is the reason why researcher added sensors to record and analyze temperature changes in safety-critical systems [9]–[13]. Vazquez et al. [10] describe in their publication the approach of a built-in an aging monitor. The monitor is implementing a redundant sensor that is only activated in car power-up and this enables the detection of aging. Another approach of Johannsson et al. [9] introduced a novel FPGA-based temperature monitoring system that is used to continously logging temperature during real-time operation. The logging data is used for estimaiting the remaining useful lifetime in a reliability tool. One drawback of the temperature logging implementation of Johannsson is the huge amount of data that needs to be collected during the system operation time of ten to fifteen years.

To establish an aging monitor in the automotive domain it is necessary to introduce an efficient temperature monitoring system that is able to record the temperature history of fifteen operation years efficiently. Strasser et al. [14] introduced a State-of-Health safety monitor that is optimized for systems in the automotive domain and is recording the temperature data efficiently in a histogram. Their method is considering the FIT Rate as a credit system that is consumed by the system and the specific cost of a point of time depends on the current system temperature. This enables the detection of a mismatch between the defined temperature mission profile and the real operation temperature profile as well as utilization deviations of the system caused by system updates [14].

To enable robust and efficient state-of-health safety monitoring for future ADAS we want to contribute on the following research work:

- Hardware Implementation of the memory efficient state-of-health safety monitor system of Strasser et al. [14] in an automotive LiDAR rapid prototyping platform including the design of a graphical front end to support mechanics and engineers to detect reliability issues.

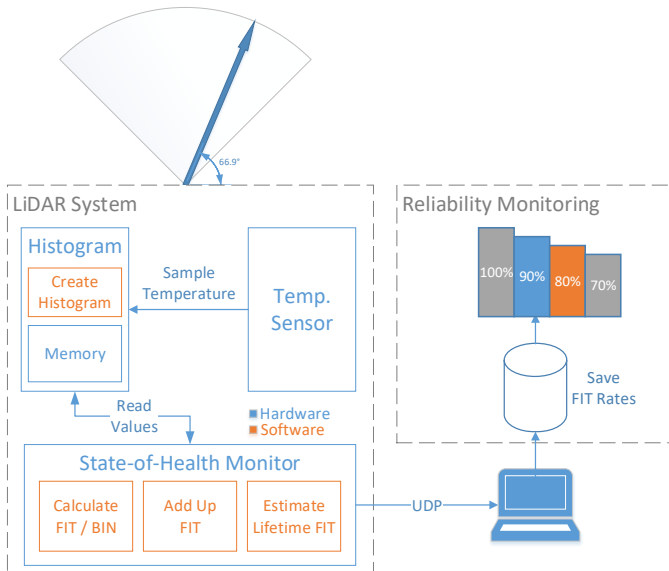


Fig. 3. Overview of the modified LiDAR system containing the state-of-health safety monitor.

III. LIVE STATE-OF-HEALTH MONITORING FOR AUTOMOTIVE LiDAR SYSTEM

In the next few years, novel automotive LiDAR system, such as the 1D MEMS Micro-Scanning LiDAR system of Druml et al. [4], will become a major key-enabler for safe and robust autonomous driving. As depicted in Figure 2, the LiDAR system is composed of the Emitter and Receiver Path in which the Emitter Path is the most safety-critical because of the MEMS Driver application-specific integrated circuit (ASIC). The MEMS Driver ASIC is responsible to sense, control and to actuate the MEMS Mirror and any failure could result in an abrupt halt of the MEMS Mirror. An abrupt halt leads to an outage of the 3D point-cloud data of the LiDAR system and in worst-case could lead to an accident. For this reason, we want to prevent such an situation of an abrupt failure of the MEMS Driver ASIC by implementing a State-of-Health Safety Monitoring system that notifies the driver in case of overstress.

A. System Architecture

In Figure 3, the adapted 1D MEMS Micro-Scanning LiDAR system can be depicted. The novel system architecture contains an additional State-of-Health (SoH) Safety Monitor that was introduced as a concept by Strasser et al. [14].

The SoH Safety Monitor is sampling the value of the internal temperature sensor at a specific frequency and maps the sampled temperature value inside a histogram, as depicted in Figure 5. The histogram is mandatory to reduce the amount of memory for the temperature logging and enables the recording of long-running data efficiently. There is a single drawback of using the histogram for logging temperature data namely loosing the chronological data of the specific temperature data; But, the chronological order of the temperature is not necessary for our use-case.

The temperature data that is sampled by the Histogram module gets further processed by the State-of-Health Monitor and calculates the estimated Lifetime Failure-In-Time Rate, the current FIT Rate and the usage Ratio.

This data can be transmitted to another system such as a workstation that is receiving the processed data over User Datagram Protocol (UDP). The UDP data is saved into a database and graphically edited to support mechanics and engineers to detect usage anomalies.

B. Mission Temperature Profile Example

Figure 4 depicts an example of a temperature mission profile of a safety-critical automotive system. The diagram illustrates the temperature distribution on the first y-axis and the related FIT Rate on the second y-axis.

For each temperature value a specific De-Rating Factor needs to be calculated as seen in (1). In due consideration of the temperature distribution and the De-Rating Factor at a specific temperature the FIT Rate at this temperature value can be calculated. The plot in Figure 4 clearly depicts that with increasing temperature the De-Rating Factor increases and further the specific FIT Rate of that temperature point.

Summing up the individual FIT Rates of each temperature value results in the overall FIT Rate of the specific safety-critical automotive system. Figure 5 depicts the histogram of the Temperature Distribution of Figure 4. The histogram is used for efficiency reasons because it requires less memory and this will save production costs.

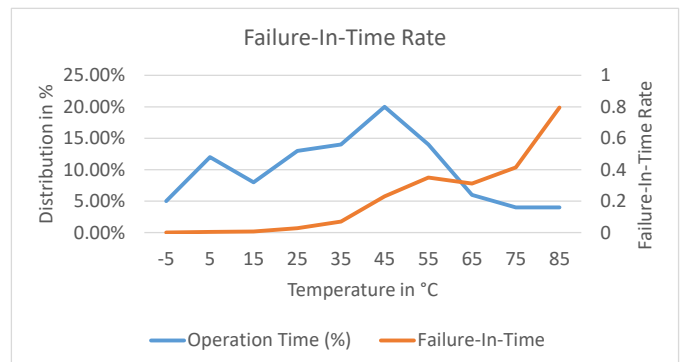


Fig. 4. Overview of the temperature distribution and the Failure-In-Time Rate at specific temperatures.

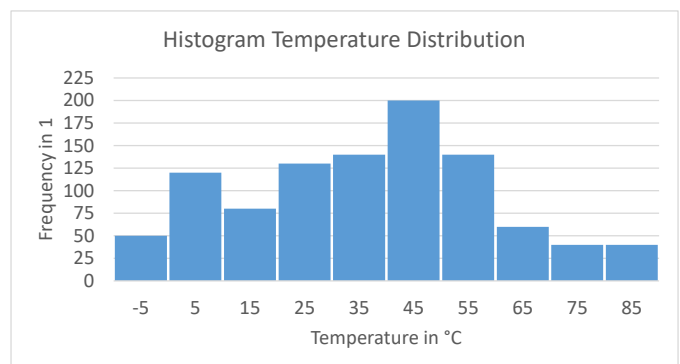


Fig. 5. Derived histogram from the operation temperature mission profile that is depicted in Figure 4.

C. Control Flow

The overall State-of-Health Monitor LiDAR platform is separated in two parts: LiDAR System and Reliability Monitor. The LiDAR system represents the rapid prototyping platform including the MEMS Driver ASIC and MEMS Mirror that is depicted in Figure 2. Additionally we have implemented the Histogram and State-of-Health Monitor modules in the LiDAR System that are illustrated in Figure 3. In general, the State-of-Health Monitor is able to calculate the estimated Lifetime FIT but for research purpose we transmit the raw histogram values to the Reliability Monitoring device over UDP. The Reliability Monitoring is responsible to process the raw histogram values and calculate the specific FIT Rates such as expected lifetime, current rate and the ratio. These processed data gets saved in a database and displayed in a specific graphical user interface (GUI) that simplifies the work of mechanics and engineers by depicting the data as graphs. Figure 6 gives a detailed overview of the asynchronous processing steps of the LiDAR System and the Reliability Monitor:

- **LiDAR System**

- 1) **Sample Temperature**

The temperature sensor is sampling the current temperature of the semiconductor device based on the sampling frequency that is set by the configuration file.

- 2) **Save Temperature Value in Histogram**

The sampled temperature value gets pre-processed by normalizing the sampling on specific temperature values such as integer values. Afterwards the value is saved inside the temperature histogram inside a non-volatile memory.

- **Reliability Monitor**

- 1) **Fetch Histogram Data**

The histogram data of the non-volatile memory that is integrated inside the LiDAR system is transmitted to the Reliability Monitor over the UDP protocol.

- 2) **Determine Current FIT Rate**

The current FIT Rate represents the currently “used” FIT. For this purpose the FIT Rate is construed as a credit system that can be consumed by the semiconductor device. Reaching a specific value that needs to be set individually for each device and depends on the ASIL as well as on the reliability requirements. Further information, especially the specific formulates, on calculating the Current FIT Rate can be consulted in publication [14]. The calculation can be separated in the following three processing steps:

- a) **Time Span Histogram Bins**

The histogram bins represents different temperature values and therefore different run-times of the system at this specific temperature. Consequently, the distribution of the individual temperature bins must be calculated considering the current operation time of the system. Based on

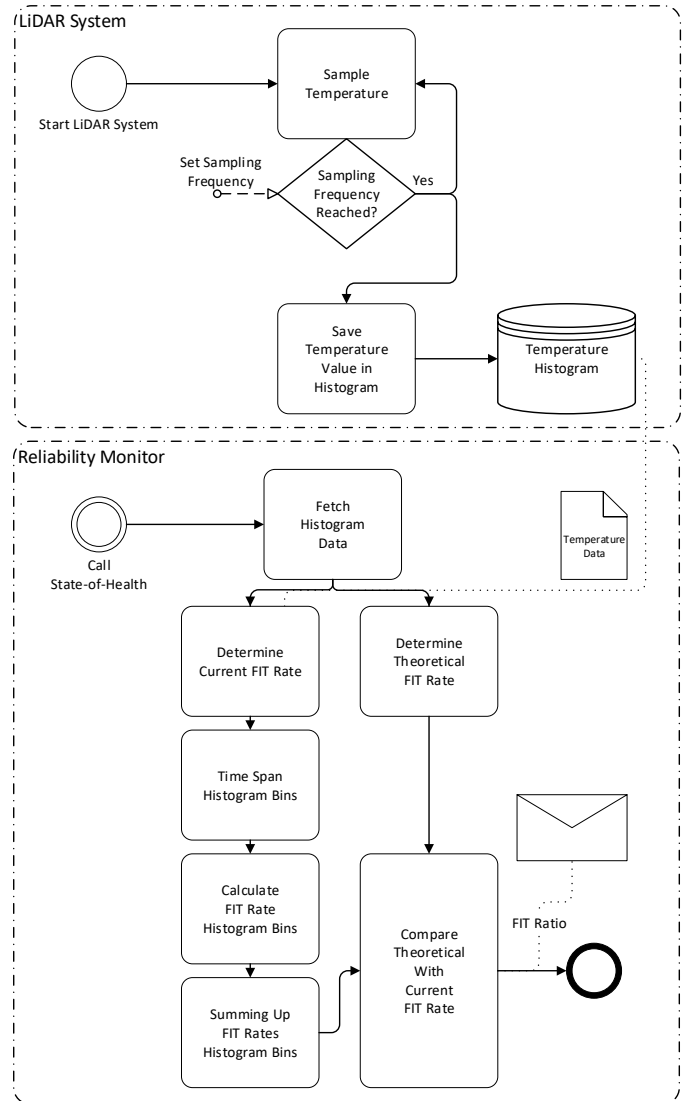


Fig. 6. Control flow of the state-of-health safety monitor that is integrated in the automotive LiDAR system.

these time spans the specific FIT Rates for each histogram bin can be calculated.

- b) **Calculate FIT Rate Histogram Bins**

Each temperature value correlates to a different De-Rating Factor as already described in equation (1). For this purpose, it is necessary to calculate the FIT Rate of each Histogram Bin separately.

- c) **Summing Up FIT Rates Histogram Bins**

In the previous processing steps the FIT Rates for each individual histogram bin, representing a specific temperature value, have been calculated. These single values are summed up to calculate the overall FIT Rate of the current operation time of the system.

- 3) **Determine Theoretical FIT Rate**

The Theoretical FIT Rate represents the approximated FIT Rate that will be reached at the end of lifetime of the safety-critical automotive LiDAR

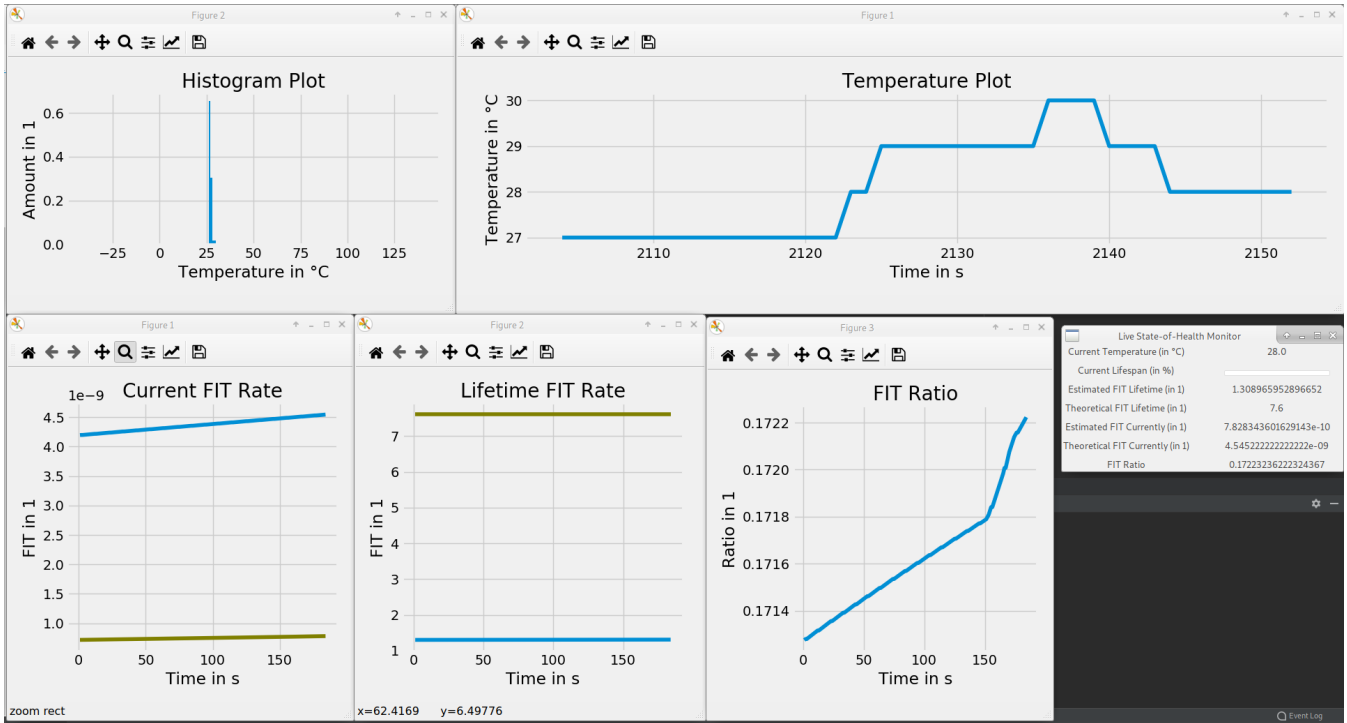


Fig. 7. Graphical User Interface of the live state-of-health monitor that was integrated in a safety-critical automotive LiDAR system.

system. This value is important to detect mismatches between the desired and indeed safety requirements and could result in an ASIL degradation.

4) Compare Theoretical With Current FIT Rate

The comparison between the theoretical and the current FIT Ratio enables a detection of overstressing the semiconductor devices. This value can be used as an alarm after software or firmware updates.

IV. RESULTS

In this section, we are presenting the practical results of the live state-of-health monitoring system that has been introduced in Section III. The novel monitoring concept was integrated into the 1D MEMS Micro-Scanning LiDAR system. The platform was heated and cooled within an environmental chamber.

Figure 7 depicts the GUI of the live state-of-health safety monitoring system that was implemented for providing reliability information to engineers and mechanics. The graphical interface provides live run-time data in diagrams as well as an overview plot of the different FIT Rates such as the current

FIT Rate. In the Temperature Plot the temperature profile that was applied to the 1D MEMS Micro-Scanning LiDAR system during the experiment can be depicted. Based on this temperature data the Histogram Plot is created and represents the complete temperature profile of the overall run-time. The Current and Lifetime FIT Rate plot represents a line for the current and theoretical value of the specific FIT Rate and is used as an optical indicator if the current FIT Rate is exceeding the designed usage of the system. Additionally, to increase the comprehensibility engineers and mechanics are also able to use the FIT Ratio that provides the possibility to detect overstress anomalies that are caused by software or firmware updates. In the FIT Ratio plot it can be seen that there was an intense increase of the FIT Rate and this can be one of the key indicators of a mismatch between the designed temperature mission profile and the real one. The data that are plotted in the diagrams are also displayed as values. These results of the experimental attempt can also be seen in Table I. The experiment resulted in an estimated lifetime FIT of about 1.3 and considering the theoretical lifetime FIT of 7.6 results in a FIT Ratio of 0.17. This ratio means that if the 1D MEMS Micro-Scanning LiDAR system operates in the same environmental conditions will result in an overdesigned system. Future redesigns of the system could be used to optimize the materials to reduce costs.

TABLE I
RESULTS OF THE EXPERIMENTAL ATTEMPT OF THE LIVE STATE-OF-HEALTH MONITOR FOR THE AUTOMOTIVE LiDAR SYSTEM.

Data	Value
Current Temperature in Degree Celsius	28.0
Estimated FIT Lifetime in 1	1.309
Theoretical FIT Lifetime in 1	7.6
Estimated FIT Currently in 1	7.23E-10
Theoretical FIT Currently in 1	4.55E-09
FIT Ratio	0.17

V. CONCLUSION

In this publication, we have introduced a novel live state-of-health safety monitoring system for a safety-critical automotive LiDAR system that will be used for autonomous driving.

One of the key-challenges was to record the reliability data efficiently and to consider the whole operation time of the system.

In Section II, we introduced the physical backgrounds of reliability in terms of semiconductor devices. Based on these physical backgrounds we provided an overview about previous research work with a similar focus of reliability monitoring. In contrast to the previous researchers, this publication focus on a reliability monitor concept that is in compliance with the automotive ISO 26262 Road vehicle safety standard. Furthermore, the work of previous researchers also did not focus on recording the reliability data efficiently.

The next Section III introduced the novel 1D MEMS Micro-Scanning LiDAR system architecture including the novel state-of-health safety monitor. For this purpose, we implemented additional modules inside the LiDAR system and an UDP interface to an external device that is responsible for fetching the reliability data and provide a graphical visualization for engineers and mechanics. A detailed overview of the control flow of both systems can be depicted in Figure 6.

The results of Section IV clearly depicts the feasibility of this monitor system and provides live reliability data of the LiDAR system. In our case, we have observed that the LiDAR system was highly robust considering the temperation mission profile of our test case. This resulted in a FIT Ratio of about 0.17 and this can be used as an indicator for redesigns possibilities to save production costs.

In the next few years, autonomous driving will disruptively change the automotive industry. In the past, the driver was the most important backup for failures but this backup solution will be missing with fully-autonomous driving vehicles. Future semiconductor devices must be highly reliable and any failures must be detected in prior to prevent hazardous situations. The novel live state-of-health monitoring system for LiDAR systems we have introduced in this publication is one solution for solving this key problem of autonomous driving. This safety monitor can also be used for any other safety-critical automotive system because of the compliance with the automotive safety standard ISO 26262.

VI. ACKNOWLEDGMENTS

The authors would like to thank all national funding authorities and the ECSEL Joint Undertaking, which funded the PRYSTINE project under the grant agreement number 783190.

PRYSTINE is funded by the Austrian Federal Ministry of Transport, Innovation and Technology (BMVIT) under the program "ICT of the Future" between May 2018 and April 2021 (grant number 865310). More information: <https://iktderzukunft.at/en/>.

REFERENCES

- [1] N. Druml, G. Macher, M. Stolz, E. Armengaud, D. Watzenig, C. Steger, T. Herndl, A. Eckel, A. Ryabokon, A. Hoess, S. Kumar, G. Dimitrakopoulos, and H. Roedig, "Prystine - programmable systems for intelligence in automobiles," in *2018 21st Euromicro Conference on Digital System Design (DSD)*, Aug 2018, pp. 618–626.
- [2] R. Faria, L. Brito, K. Baras, and J. Silva, "Smart mobility: A survey," in *2017 International Conference on Internet of Things for the Global Community (IoTGC)*, July 2017, pp. 1–8.
- [3] N. Lang, M. Rüßmann, A. Mei-Pochtler, T. Dauner, S. Komiya, X. Mosquet, and X. Doubara, "Self-driving vehicles, robo-taxis, and the urban mobility revolution," *The Boston Consulting Group*, vol. 7, p. 2016, 2016.
- [4] N. Druml, I. Maksymova, T. Thurner, D. Van Lierop, M. Hennecke, and A. Foroutan, "1D MEMS Micro-Scanning LiDAR," in *Conference on Sensor Device Technologies and Applications (SENSORDEVICES)*, 09 2018.
- [5] J. Hecht, "Lidar for self-driving cars," *Optics and Photonics News*, vol. 29, no. 1, pp. 26–33, 2018.
- [6] I. n. E. ISO, "Draft 26262 2nd Edition: Road vehicles-Functional safety," *International Standard ISO/FDIS*, vol. 26262, 2018.
- [7] D.-G. Yang, F. Wan, Z. Shou, W. D. van Driel, H. Scholten, L. Goumans, and R. Faria, "Effect of high temperature aging on reliability of automotive electronics," *Microelectronics Reliability*, vol. 51, no. 9-11, pp. 1938–1942, 2011.
- [8] T. IEC, "62380," *Reliability data handbook—universal model for reliability prediction of electronics components, PCBs and equipment (emerged from UTEC 80-810 or RDF 2000)*, 2004.
- [9] C. Johansson, J. Arwidson, and T. Månefjord, "An fpga-based monitoring system for reliability analysis," in *Additional Conferences (Device Packaging, HiTEC, HiTEN, & CICMT)*, vol. 2017, no. NOR. International Microelectronics Assembly and Packaging Society, 2017, pp. 1–4.
- [10] J. C. Vazquez, V. Champac, A. Ziesemer, R. Reis, I. C. Teixeira, M. B. Santos, and J. P. Teixeira, "Built-in aging monitoring for safety-critical applications," in *2009 15th IEEE International On-Line Testing Symposium*. IEEE, 2009, pp. 9–14.
- [11] K. Arabi and B. Kaminska, "Built-in temperature sensors for on-line thermal monitoring of microelectronic structures," in *Proceedings International Conference on Computer Design VLSI in Computers and Processors*. IEEE, 1997, pp. 462–467.
- [12] S. Majerus, X. Tang, J. Liang, and S. Mandal, "Embedded silicon odometers for monitoring the aging of high-temperature integrated circuits," in *2017 IEEE National Aerospace and Electronics Conference (NAECON)*. IEEE, 2017, pp. 98–103.
- [13] M. Civilini, "Reliability and field aging time using temperature sensors," in *2010 Fourth International Conference on Sensor Technologies and Applications*. IEEE, 2010, pp. 210–213.
- [14] A. Strasser, P. Stelzer, C. Steger, and N. Druml, "Live state-of-health safety monitoring for safety-critical automotive systems," in *2019 22nd Euromicro Conference on Digital System Design (DSD)*, Aug 2019.